[1] a) J. J. Turner, *Endeavour* **1968**, *27*, 42 – 47; b) D. Königstein, M. Jansen, *Monatsh. Chem.* **1996**, *127*, 1221 – 1227; c) T. Bremm, M. Jansen, *Z. Anorg. Allg. Chem.* **1992**, *610*, 64 – 66.
[2] a) D. Y. Naumov, A. V. Virovets, N. V. Podberezskaya, P. B. Novikov, A. A. Politov, *J. Struct. Chem.* **1997**, *38*, 772 – 778; b) W. P. Griffith, R. D. Powell, A. C. Skapski, *Polyhedron* **1988**, *7*, 1305 – 1310.
[3] a) E. J. Constam, A. von Hansen, *Z. Elektrochem.* **1896**, *7*, 137 – 144; b) A. von Hansen, *Z. Elektrochem.* **1896**, *7*, 445 – 448; c) A. K. Melnikov, T. P. Firsova, A. N. Molodkina, *Russ. J. Inorg. Chem.* **1962**, *7*, 637 – 640; d) P. A. Giguère, D. Lemaire, *Can. J. Chem.* **1972**, *50*, 1472 – 1477; e) D. P. Jones, W. P. Griffith, *J. Chem. Soc. Dalton Trans.* **1980**, 2526 – 2532.
[4] Early X-ray powder diffraction erperiments have been reported, which failed to find the correct unit cell and X-ray density.[5]
[5] V. I. Sokol, V. M. Bakulina, E. Y. Filatov, T. P. Firsova, *Russ. J. Inorg. Chem.* **1968**, *13*, 1211 – 1212.
[6] a) E. H. Riesenfeld, B. Reinhold, *Ber. Dtsch. Chem. Ges.* **1909**, *42*, 4377 – 4383; b) J. M. Adams, R. G. Pritchard, *Acta Crystallogr. Sect. B* **1977**, *33*, 3650 – 3653.
[7] a) A. Adam, M. Mehta, *Angew. Chem.* **1998**, *110*, 1457 – 1459; *Angew. Chem. Int. Ed.* **1998**, *37*, 1387 – 1388; b) A. Adam, M. Mehta, *Z. Kristallogr.* **1998**, *Supplement Issue 15*, 46.
[8] Interpretation of the IR data was based on the wrong molecular symmetry; however, the postulation of a peroxodicarbonate anion was correct.[3e]
[9] a) Crystal structure data of $K_2C_2O_6$: monoclinic, space group $P2_1/c$ (no. 14), $a = 838.05(1)$, $b = 1076.41(2)$, $c = 711.67(1)$ pm, $\beta = 111.24(0)^\circ$ $V = 598.4(2) \times 10^6$ pm^3, $\rho_{calcd} = 2.200$ g cm^{-3}, $\rho_{measured} = 2.14(1)$ g cm^{-3} (He pycnometer, Micrometritics AccuPyc 1330 GB), $Z = 4$, $\mu = 55.04$ cm^{-1}. b) Devices for X-ray diffraction experiments: Suny X3B1 beamline at National Synchroton Light Source, Brookhaven National Laboratory, USA, double Si(111) monochromator, and Ge(111) crystal analyzer, $\lambda = 115.011(2)$ pm, Na(Tl)I scintillation counter with pulse height discriminator, $T = -73\,^\circ$C, $5.0^\circ < 2\Theta < 43.679^\circ$ in steps of $0.003^\circ 2\Theta$, glass capillary of 0.7 mm diameter; due to decomposition even at low temperature, a second measurement for structure refinement was performed at beamline B2 at the Hamburger Synchrotronstrahlungslabor (HASYLAB) immediately after synthesis of the material: Three-circle Huber goniometer, Ge(111) double crystal monochromator, and Ge(111) crystal analyzer, $\lambda = 112.074(2)$ pm, Na(Tl)I scintillation counter, $T = -123\,^\circ$C, $9.0^\circ < 2\Theta < 50.5^\circ$ in steps of $0.003^\circ 2\Theta$, glass capillary of 0.7 mm diameter. c) Structure determination process: Data reduction and background modeling by using the GUFI program,[10] crystal structure solution by global optimization with 15 parameters by using the DASH program package,[11] two phases of Rietveld refinements by employing a model for anisotropic micro-strain with potassium hydrogencarbonate as second phase by using the GSAS program package,[12] $R_p = 0.193$, $R_{wp} = 0.246$, $R_F = 0.080$, $\chi^2 = 0.84$, number of reflections 281, number of variables 35, number of refined atoms 10. The relatively high weighted-profile R factor is due to the statistics of the observed step scan intensities caused by limited time for measurement. d) Further details on the crystal structure investigation may be obtained from the Fachinformationszentrum Karlsruhe, 76344 Eggenstein-Leopoldshafen, Germany (fax: (+49) 7247-808-666; e-mail: crysdata@fiz-karlsruhe.de), on quoting the depository number CSD-412335.
[10] R. Dinnebier, GUFI a program for measurement and evaluation of powder patterns, Version 5.0, Heidelberger Geowiss. Abh. 68, Heidelberg, **1997**.
[11] a) W. I. F. David, K. Shankland, N. Shankland, *Chem. Commun.* **1998**, 931 – 932; b) J. W. Visser, *J. Appl. Crystallogr.* **1969**, *2*, 89 – 95; c) A. Le Bail, H. Duroy, J. L. Fourquet, *Mater. Res. Bull.* **1988**, *23*, 447 – 452; d) J. Rodriguez-Carvajal, *Abstracts of the Satellite Meeting on Powder Diffraction of the XV Congress of the IUCR*, **1990**, p. 127.
[12] a) A. C. Larson, R. B. von Dreele, *GSAS* **1990**, Version Sept. 1997, Los Alamos National Laboratory Report LAUR 86 – 748; b) H. M. Rietveld, *J. Appl. Crystallogr.* **1969**, *2*, 65 – 71; c) P. Thompson, D. E. Cox, J. B. Hastings, *J. Appl. Crystallogr.* **1987**, *20*, 79 – 83; d) L. W. Finger, D. E. Cox, A. P. Jephcoat, *J. Appl. Crystallogr.* **1994**, *27*, 892 – 900; e) P. W. Stephens, *J. Appl. Crystallogr.* **1999**, *281 – 289*.
[13] Molecular calculations (MINDO), in which C_2 symmetry was assumed for the peroxodicarbonate group, failed to correctly postulate the bond lengths and the dihedral angle.[14]
[14] C. Glidewell, *J. Mol. Struct.* **1980**, *67*, 35 – 44.
[15] a) J.-M. Savariault, M. S. Lehmann, *J. Am. Chem. Soc.* **1980**, *102*, 1298 – 1303; b) Y. Idemoto, J. W. jr. Richardson, N. Koura, S. Kohara, C.-K. Loong, *J. Phys. Chem. Solids* **1998**, *59*, 363 – 376; A. Y. Kosnikov, V. L. Antonovsky, S. V. Lindeman, Y. T. Struchkov, I. P. Zyatkov, *Kristallografiya* **1988**, *33*, 875 – 877.
[16] G. Jander, K. F. Jahr, *Maßanalyse*, 15th ed., de Gruyter, Berlin, **1989**, pp. 197 – 198.

Self-Assembled Receptors for Enantioselective Recognition of Chiral Carboxylic Acids in a Highly Cooperative Manner

Tsutomu Ishi-i, Mercedes Crego-Calama, Peter Timmerman,* David N. Reinhoudt,* and Seiji Shinkai

One of the ultimate aims in molecular recognition is to understand fully and mimic the exquisite selectivities so eminently observed in natural receptors, such as antibodies and enzymes. A first approach is to build synthetic receptors by using rigid covalent scaffolds, to which are attached functional groups that can bind their guest molecules by multiple noncovalent interactions, such as hydrogen bonding, $\pi - \pi$ stacking, or metal coordination.[1] However, covalent systems are often too rigid and unable to adapt their shape to that of the guest, which can result in less than optimal binding affinities and selectivities. Another important drawback of covalent receptor molecules is their labor-intensive synthesis, which leaves little potential for structural variations in the scaffold.[2]

A different approach to shaping the binding site of an artificial receptor is to bring together the different components by multiple noncovalent interactions.[3, 4] This approach, which more closely resembles Nature's strategy, is currently being investigated as a potential alternative to covalent receptor molecules. A number of systems based on coordinative metal – ligand interactions[5] or hydrogen-bonding interactions[6] have been investigated, and some show significant structural selectivities.[7] However, in the majority of cases, substrate selectivity is the result of shape complementarity

[*] Dr. P. Timmerman, Prof. Dr. Ir. D. N. Reinhoudt, Dr. T. Ishi-i, Dr. M. Crego-Calama
Laboratory of Supramolecular Chemistry and Technology
MESA$^+$ Research Institute, University of Twente
PO Box 217, 7500 AE Enschede (The Netherlands)
Fax: (+31) 53-4894645
E-mail: d.n.reinhoudt@ct.utwente.nl
Prof. Dr. S. Shinkai
Chemotransfiguration Project
Japan Science and Technology Corporation (Japan)

Supporting information for this article is available on the WWW under http://www.angewandte.com or from the author.

  1433-7851/02/4111-1924 $ 20.00+.50/0

rather than specific binding. Strong coordinative metal–ligand interactions have been used for the synthesis of receptors with specific binding of guest molecules.[4] Nevertheless, hydrogen-bonded, self-assembled receptors which bind the guest through functional-group interactions are rare,[8] probably because such functionalities are often not compatible with the noncovalent interactions that hold the receptor together.[3] Here we show that amino functionalities positioned on a chiral noncovalent scaffold stereospecifically recognize carboxylic acids with detailed structural selectivities, both with respect to the substrate and the scaffold. The recognition takes place primarily by use of acid–base (NH_2–HOOC) interactions,[9–12] whereas the observed enantioselectivity is the result of a secondary interaction with the noncovalent platform, which acts in a cooperative manner, similar to the binding of oxygen in hemoglobin.

The core of the self-assembled scaffold consists of a double-rosette hydrogen-bonded assembly $\mathbf{1}_3 \cdot (CYA)_6$ (CYA = cyanuric acid), to which six amino functionalities have been attached; these serve as principal binding sites for guest complexation. The scaffold is composed of nine different components, that is, three calix[4]arene dimelamines **1** and six units of a barbituric or cyanuric acid derivative.[13] A total of 36 cooperative hydrogen bonds hold the components together, so that these structures are fully assembled at $>5\ \mu M$ in benzene or at $>100\ \mu M$ in chloroform.[14] The scaffold can be present in three isomeric forms (D_3, C_s, and C_{3h}), of which the chiral D_3 isomer is formed in most cases.[15] When no chiral centers are present in either one of the components, the D_3 isomer exists as a racemic mixture of the *P* and *M* enantiomers (Figure 1). However, chiral centers present in either **1** or CYA induce the supramolecular chirality of the scaffold, and only one of the two diastereoisomers (*P* or *M*) is formed.[16] Assembly $\mathbf{1}_3 \cdot (CYA)_6$ is strongly circular-dichroism (CD) active because of the dissymmetric arrangement of the many different chromophoric units within the structure.[14]

We studied the complex formation of double-rosette assembly $\mathbf{1a}_3 \cdot (CYA)_6$ (R = 2,2-dimethylpropyl amine)[17] with a variety of chiral carboxylic acids **2**. The assembly $\mathbf{1a}_3 \cdot (CYA)_6$ is used as a platform to organize the six amino functionalities. Typically, six equivalents of **2** were added to a solution of $\mathbf{1a}_3 \cdot (BuCYA)_6$ (1.0 mM) in [D_8]toluene at room temperature (ratio of COOH:NH_2 1:1) and the mixtures were equilibrated for ten hours. The interaction between host and guest becomes apparent from shifts of the signals in the ^1H NMR spectrum (Figure 2). For example, in the case of acid (*S*)-**2b** (6 equiv), the H^k (2.57 ppm) and H^l (2.37 ppm) proton signals shift upfield and downfield $-(0.09-0.18$ ppm) and $+0.32$ ppm, respectively, upon addition of the guest (Figure 3). In addition, signals for the H^b, H^c, H^k, and H^l protons are split, because of the formation of the diastereomeric assemblies (*M*)-$\mathbf{1a}_3 \cdot (BuCYA)_6$/(*S*)-**2b** and (*P*)-$\mathbf{1a}_3 \cdot (BuCYA)_6$/(*S*)-**2b**, which are no longer mirror images (Figure 2 and 3).[18] In contrast, (*S*)-**2b** shows no interaction with assembly $\mathbf{1d}_3 \cdot (BuCYA)_6$, which

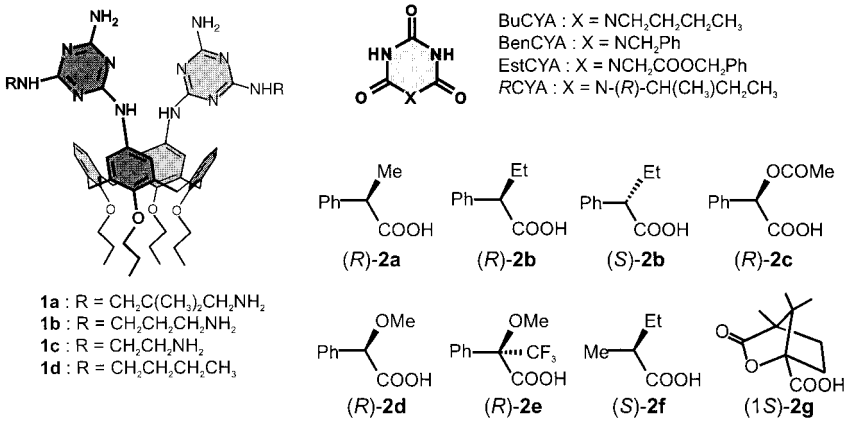

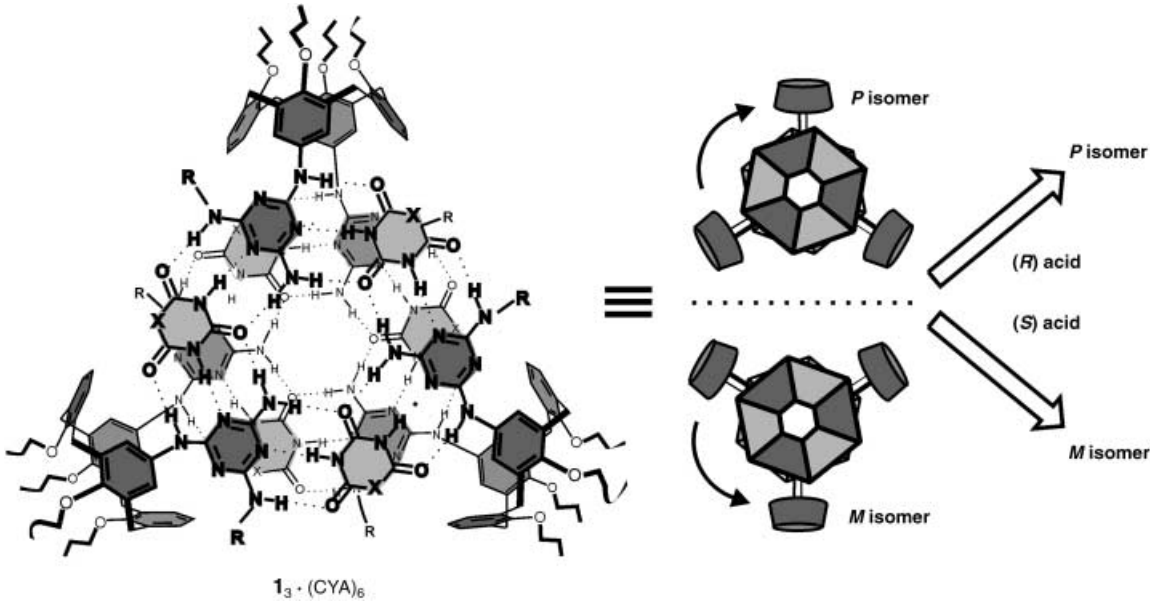

Figure 1. Chiral recognition by D_3-symmetrical rosette assemblies.

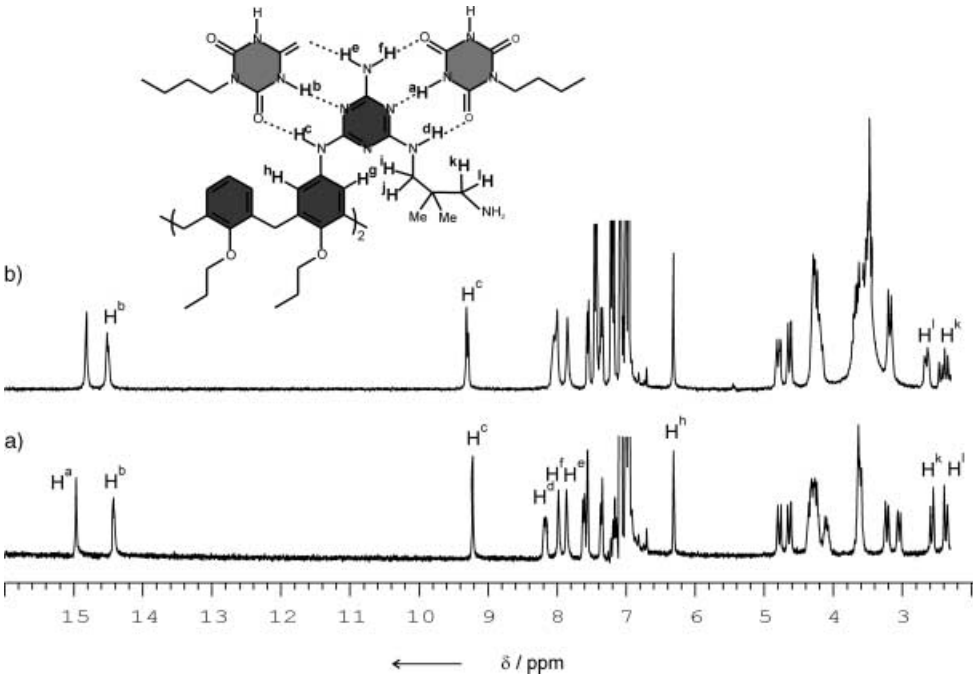

Figure 2. ^{1}H NMR spectra of $\mathbf{1a}_3\cdot(\mathrm{BuCYA})_6$ (1 mM) in [D_8]toluene in the presence of a) none and b) six equivalents of (*S*)-**2b**.

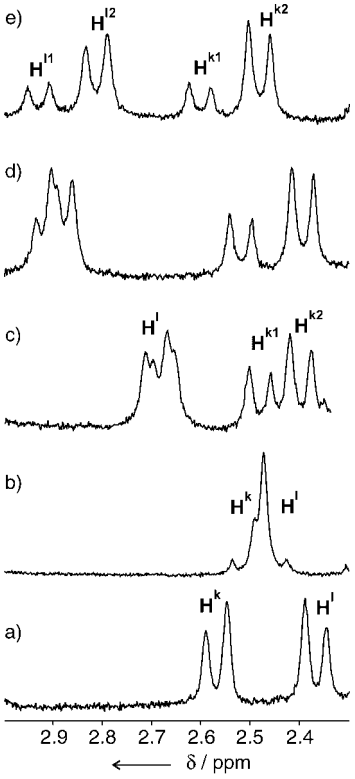

Figure 3. H^k and H^l proton resonance signals in the ^{1}H NMR spectra of $\mathbf{1a}_3\cdot(\mathrm{BuCYA})_6$ in the presence of (*S*)-**2b**: in [D_8]toluene, [$\mathbf{1a}_3\cdot(\mathrm{BuCYA})_6$] = 1 mM: a) 0, b) 1.5, c) 6, d) 12, and e) 60 equivalents of (*S*)-**2b**.

lacks the pendant amino groups. Complexation-induced shifts were not observed in this case, even when (*S*)-**2b** was present in a large excess (≈90 equiv), which clearly indicates that (*S*)-**2b** interacts primarily with the pendant amino group in $\mathbf{1a}_3\cdot(\mathrm{BuCYA})_6$.

The chiral acids (*R*)-**2a**, (*R*)-**2b**, (*S*)-**2b**, (*R*)-**2c**, (*S*)-**2f**, and (1*S*)-**2g** express a clear selectivity in binding towards one of the two enantiomers (*M* or *P*) of assembly $\mathbf{1a}_3\cdot(\mathrm{BuCYA})_6$. As a result, the enantiomer that is bound most strongly is amplified in the mixture, as both enantiomers are in dynamic equilibrium. This increase causes the CD spectrum of assembly $\mathbf{1a}_3\cdot(\mathrm{BuCYA})_6$ to show reliable and reproducible Cotton effects in the presence of these chiral acids (Figure 4). The corresponding *de* values can be determined by measuring the peak intensities for both diastereomeric complexes in the ^{1}H NMR spectrum: for the complexation with (*S*)-**2b** (>12 equiv), the *de* values were directly estimated by integration of the completely split

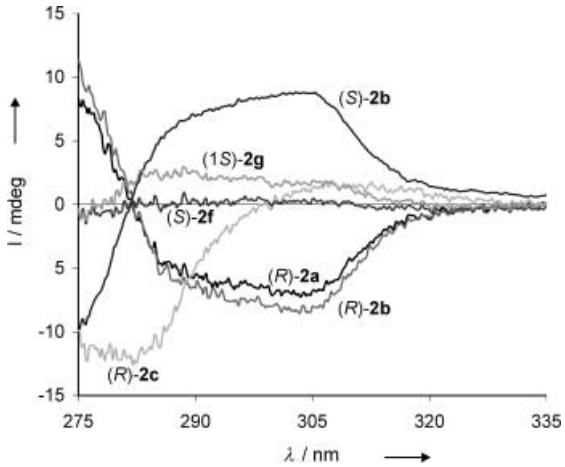

Figure 4. CD spectra of $\mathbf{1a}_3\cdot(\mathrm{BuCYA})_6$ (1 mM) in [D_8]toluene in the presence of (*R*)-**2a**, (*R*)-**2b**, (*S*)-**2b**, (*R*)-**2c**, (*S*)-**2f**, and (1*S*)-**2g** (6 equiv; in 0.01-cm-width cell).

signals arising from H^{k1} and H^{k2} (Figure 3). Under the optimum conditions (60 equivalents of (*S*)-**2b**, Figure 3e) a *de* value of 50% can be achieved. A plot of these values against the CD intensities at 305 nm (see Supporting Information) gives a straight line, from which an ellipticity of ~36 mdeg ($\Delta\varepsilon \sim 110\ \mathrm{cm^2\,mmol^{-1}}$) can be determined at 100% *de*, by extrapolation from the data. This value compares well with CD intensities of diastereomerically pure rosette assemblies.[17] This relationship allows us to calculate *de* values directly from the CD spectra (Table 1), because the *de* values could be obtained directly from ^{1}H NMR titration methods in (*S*)-**2f** and (1*S*)-**2g** systems.

The enantioselectivity differs strongly amongst the various chiral acids **2**. The highest enantioselectivities were observed

  1433-7851/02/4111-1926 $ 20.00+.50/0 *Angew. Chem. Int. Ed.* **2002**, *41*, No. 11

Table 1. Induction of chirality in assembly $\mathbf{1a}_3 \cdot (\mathrm{BuCYA})_6$ as a result of the addition of chiral acids **2a**–**g**.[a]

Entry	**2**	Yield [b] [%]	*de* value [d] [%]	Helicity[f]	CD_{305} [g] [mdeg]
1	–	100	–	–	–
2	(*R*)-**2a**	100	19	*P*	– 6.79
3	(*R*)-**2b**	100	21	*P*	– 7.80
4	(*S*)-**2b**	100	21	*M*	7.73
5	(*R*)-**2c**	54	[e]	–	– 12.6[h]
6	(*R*)-**2d**	[c]	–	–	–
7	(*R*)-**2e**	[c]	–	–	–
8	(*S*)-**2f**	100	1	*M*	0.43
9	(1*S*)-**2g**	55	5	*M*	1.87

[a] Conditions: in [D_8]toluene, $[\mathbf{1a}_3 \cdot (\mathrm{BuCYA})_6] = 1.0$ mM, $[\mathbf{2}]/[\mathbf{1a}_3 \cdot (\mathrm{BuCYA})_6] = 6$, at room temperature. [b] Determined by integration of the $ArCH_2Ar$ and the NH/ArH^h proton signals in the ^1H NMR spectrum. [c] Precipitate was formed upon addition of the acid. [d] Calculated from the CD signal intensity at 305 nm (see Supporting Information). [e] The *de* value could not be checked because of the different CD pattern and lack of splitting in the ^1H NMR spectrum. [f] Helicity of the preferentially formed isomer (*M* or *P*) of assembly $\mathbf{1a}_3 \cdot (\mathrm{BuCYA})_6$, which is assigned on the basis of CD signal sign: see reference [16]. [g] CD signal intensity at 305 nm. [h] CD signal intensity at 282 nm.

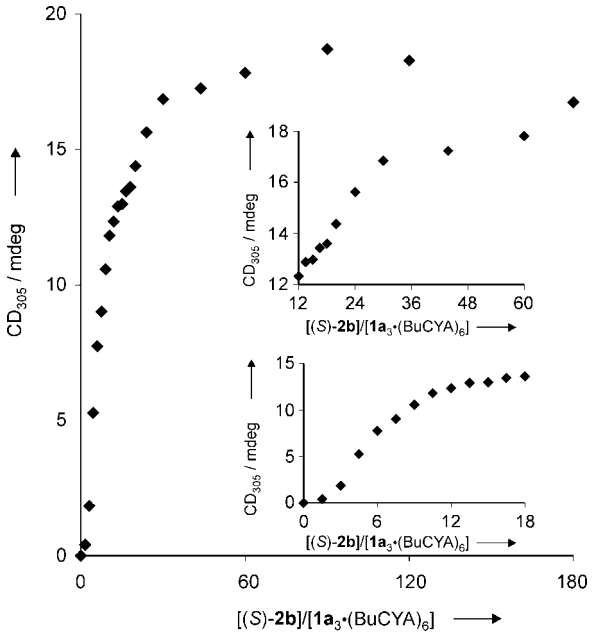

Figure 5. Plot of CD values at 305 nm versus $[(S)\text{-}\mathbf{2b}]/[\mathbf{1a}_3 \cdot (\mathrm{BuCYA})_6]$ for the titration of $\mathbf{1a}_3 \cdot (\mathrm{BuCYA})_6$ by (*S*)-**2b** in [D_8]toluene; $[\mathbf{1a}_3 \cdot (\mathrm{BuCYA})_6] = 1$ mM. The insets show expansions of the main plot.

for acids **2a** and **2b**, that is, 19 and 21 % *de* (6 equiv, entries 2–4 in Table 1). However, a drastic decrease in *de* value (to ≈1 %) was observed upon substitution of the phenyl for a methyl group, as in **2f** (compare entries 3 and 4 with 8 in Table 1), emphasizing the crucial importance of the phenyl group in the chiral recognition process. The acids (*R*)-**2c** and (1*S*)-**2g** seem to break down the scaffold, while complex formation occurs (entries 5 and 9 in Table 1). Interestingly, the CD spectrum in the presence of (*R*)-**2c** is entirely different from the others (Figure 4), which may suggest that the assembly changes structure upon binding to (*R*)-**2c**. On the addition of the acids (*R*)-**2d** and (*R*)-**2e**, a white precipitate was immediately formed (entries 6 and 7 in Table 1), which precludes solution studies on these systems. ^1H NMR spectroscopic analysis ([D_6]DMSO) shows that for (*R*)-**2d**, the hexameric complex $\mathbf{1a}_3 \cdot (\mathrm{BuCYA})_6 \cdot [(R)\text{-}\mathbf{2d}]_6$ precipitates (molar ratio of 1:2:2 for **1a**:BuCYA:(*R*)-**2d**).

Interestingly, the observed CD signals are strongly dependent on the amount of chiral acid **2** present. It is likely that the *de* value will increase with an increasing number of chiral acid units in the complex.[16] Indeed, titration of assembly $\mathbf{1a}_3 \cdot (\mathrm{BuCYA})_6$ against (*S*)-**2b** clearly shows a nonlinear increase in the CD intensity at 305 nm. First, the CD intensity increases by up to 90 times and then slowly decreases upon further addition of (*S*)-**2b** (Figure 5). The observed CD spectrum changes clearly indicate two saturation points around 15 equivalents and 60 equivalents, which suggests a two-step mechanism for the complex formation. An isosbestic point observed in both the first and second complexation indicates that only two species are present in each equilibrium (see Supporting Information). Interestingly, both the first and second CD spectra display sigmoidal curvatures; this curvature is a sign of homotropic positive allosterism, which arises from cooperativity in the complexation process.[10, 19] The cooperativity was analyzed using Equation (1)

$$y = K/([G]^{-n} + K) = \mathrm{CD_{obs}}/\mathrm{CD_{sat}} \quad (1)$$

and the Hill equation [Eq. (2)],[20] where [*G*] is the concentration of the added guest (*S*)-**2b**, *K* the association constant, *n* the Hill coefficient, $\mathrm{CD_{obs}}$ the observed CD intensity, and $\mathrm{CD_{sat}}$ the saturated CD intensity.

$$\log(y/(1-y)) = n \log[G] + \log K \quad (2)$$

From a plot of $\log(y/(1-y))$ against $\log[G]$, values of $\log K = 6.6$ and $n = 2.9$ were calculated for the first sigmoidal CD change (correlation coefficient, 0.996). For the second sigmoidal change, values of $\log K = 4.1$ and $n = 2.1$ (correlation coefficient, 0.995) were obtained (for details see Supporting Information).[21] These *n* values suggest that three molecules of (*S*)-**2b** interact with the three amino groups on one side of assembly $\mathbf{1a}_3 \cdot (\mathrm{BuCYA})_6$, to form the 1:3 complex $\mathbf{1a}_3 \cdot (\mathrm{BuCYA})_6 \cdot [(S)\text{-}\mathbf{2b}]_3$, whereupon three additional molecules of (*S*)-**2b** interact with the remaining three amino groups at the other side to form the 1:6 complex $\mathbf{1a}_3 \cdot (\mathrm{BuCYA})_6 \cdot [(S)\text{-}\mathbf{2b}]_6$.[22] In each step, the three amino groups interact with (*S*)-**2b** in a cooperative way.

The observed selectivity for complexation of chiral acid **2b** is very sensitive to structural changes in the hydrogen-bonded scaffold. For example, replacement of the 2,2-dimethyl-1,3-propylene linkers in **1a** with 1,3-propylene (**1b**) or ethylene (**1c**) spacers completely inhibits complex formation. Instead, the corresponding assemblies $\mathbf{1b}_3 \cdot (\mathrm{BuCYA})_6$ and $\mathbf{1c}_3 \cdot (\mathrm{BuCYA})_6$ are not stable and dissociate in the presence of (*R*)-**2b** (6 equiv). Similarly, the selectivities change dramatically when BuCYA is replaced with BenCYA or EstCYA. Despite the complete stability of the corresponding assemblies $\mathbf{1a}_3 \cdot (\mathrm{BenCYA})_6$ and $\mathbf{1a}_3 \cdot (\mathrm{EstCYA})_6$ in [D_8]toluene in the presence of (*R*)-**2b** (6 equiv), the observed *de* value decreases to 0 %. Most remarkable is the observation that

  1433-7851/02/4111-1927 $ 20.00+.50/0

addition of six equivalents of (*R*)-**2b** to the chiral assembly (*P*)-$\mathbf{1a}_3\cdot(\mathrm{RCYA})_6$, which bears an additional methyl group on the α-carbon of the propyl chain, leads to almost complete loss of optical activity (assembly formation decreased to about 50% and CD intensity at 305 nm decreased to about 10%). These results clearly illustrate how sensitive the observed enantioselectivity is to structural changes, which emphasizes once more the subtle nature of this particular complexation process.

How exactly does **2b** interact with the chiral assembly $\mathbf{1a}_3\cdot(\mathrm{BuCYA})_6$? The interaction is primarily electrostatic in nature, as **2b** transfers a proton to the basic amino group. The tight ion pair is the main species.[23] According to computer simulations of the hexacation $\mathbf{1a}_3\cdot(\mathrm{BuCYA})_6\cdot(\mathrm{H}^+)_6$ (gas phase MM calculation, Quanta 97/CHARMm 24.0; Figure 6), it is possible that the pendant

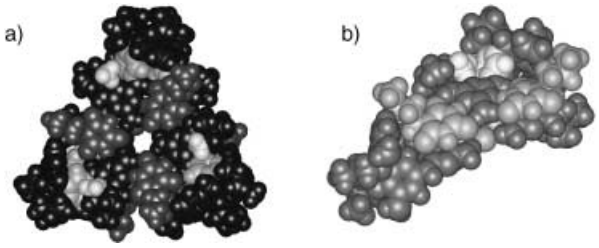

Figure 6. Computer-simulated structure of a) hexacation $\mathbf{1a}_3\cdot(\mathrm{BuCYA})_6\cdot(\mathrm{H}^+)_6$ and b) close-up (only half of the structure is shown for clarity).

NH_3^+ groups interact strongly with the electron-rich aromatic ring in the connecting calix[4]arene moiety, through cation–π interactions (Figure 6).[24, 25] The calculated distances between the NH^+ nitrogen atom and the aromatic carbon atoms (NH^+–ArC; 3.0–3.7 Å) are very close to those of the benzene–ammonia dimer (distance N–benzene plane = 3.59 Å), as measured by spectroscopy.[26] This interaction induces a significant conformational change in the scaffold and removes any rotational freedom within the binding site. The fixed RNH_3^+ functionalities are in a chiral environment and adopt a clearly defined spatial orientation to recognize chiral guests enantioselectively. The strong RNH_3^+–benzene interaction also accounts for the observed cooperativity, because the binding of one molecule of **2** will strongly preorganize and fix the binding site for the second, third, etc. molecules of **2**,[19] as the various binding sites are interconnected by the noncovalent scaffold. It seems likely that attractive guest–guest interactions[27] (for example, face-to-face or edge-to-face π–π stacking) might also contribute to the observed cooperativity, with regards to the drastic decrease in enantioselectivity from **2b** to **2f**.[28]

In conclusion, we have demonstrated that noncovalent hydrogen-bonded assemblies are able to recognize chiral carboxylic acids by a simple acid–base complexation, with considerable structural and stereoselectivities. Cooperativity in the binding process probably plays an important role in the observed selectivities, which are very sensitive to changes in the structure of the host.

Received: February 4, 2002 [Z18639]

[1] *Comprehensive Supramolecular Chemistry* (Eds.: J.-M. Lehn, J. L. Atwood, J. E. D. Davies, D. D. MacNicol, F. Vögtle), Pergamon, Oxford, **1996**.

[2] A. Fürer, T. Marti, F. Diederich, H. Künzer, M. Brehm, *Helv. Chim. Acta* **1999**, *82*, 1843–1859.

[3] a) M. M. Conn, J. Rebek, Jr., *Chem. Rev.* **1997**, *97*, 1647–1668; b) J. Rebek, Jr., *Acc. Chem. Res.* **1999**, *32*, 278–286; c) J. Rebek, Jr., *Chem. Commun*. **2000**, 637–643.

[4] a) M. S. Goodman, V. Jubian, B. Linton, A. D. Hamilton, *J. Am. Chem. Soc*. **1995**, *117*, 11610–11611; b) B. Linton, A. D. Hamilton, *Chem. Rev*. **1997**, *97*, 1669–1680.

[5] a) M. Fujita, *Chem. Soc. Rev*. **1998**, *27*, 417–425; b) D. L. Caulder, K. N. Raymond, *Acc. Chem. Res*. **1999**, *32*, 975–982; c) D. L. Caulder, K. N. Raymond, *J. Chem. Soc. Dalton Trans*. **1999**, 1185–1200; d) M. Fujita, K. Umemoto, M. Yoshizawa, N. Fujita, T. Kusukawa, K. Biradha, *Chem. Commun*. **2001**, 509–518.

[6] T. Heinz, D. M. Rudkevich, J. Rebek, Jr., *Nature* **1998**, *394*, 764–766.

[7] a) J. Kang, J. Rebek, Jr., *Nature* **1997**, *385*, 50–52; b) T. Kusukawa, M. Yoshizawa, M. Fujita, *Angew. Chem*. **2001**, *113*, 1931–1936; *Angew. Chem. Int. Ed*. **2001**, *40*, 1879–1884.

[8] a) Counteranion recognition by cation-templated assemblies: X. Shi, J. C. Fettinger, J. T. Davis, *Angew. Chem*. **2001**, *113*, 2909–2913; *Angew. Chem. Int. Ed*. **2001**, *40*, 2827–2831; b) tripyridine-templated assembly by metal–ligand interaction: M. Crego-Calama, P. Timmerman, D. N. Reinhoudt, *Angew. Chem*. **2000**, *112*, 771–774; *Angew. Chem. Int. Ed*. **2000**, *39*, 755–758.

[9] E. Yashima, K. Maeda, Y. Okamoto, *Nature* **1999**, *399*, 449–451.

[10] a) M. Takeuchi, T. Imada, S. Shinkai, *Angew. Chem*. **1998**, *110*, 2242–2246; *Angew. Chem. Int. Ed*. **1998**, *37*, 2096–2099; b) M. Ikeda, M. Takeuchi, A. Sugasaki, A. Robertson, T. Imada, S. Shinkai, *Supramol. Chem*. **2000**, *12*, 321–345.

[11] Y. Furusho, T. Kimura, Y. Mizuno, T. Aida, *J. Am. Chem. Soc*. **1997**, *119*, 5267–5268.

[12] Y. Inai, K. Tagawa, A. Takasu, T. Hirabayashi, T. Oshikawa, M. Yamashita, *J. Am. Chem. Soc*. **2000**, *122*, 11731–11732.

[13] P. Timmerman, R. H. Vreekamp, R. Hulst, W. Verboom, D. N. Reinhoudt, K. Rissanen, K. A. Udachin, J. Ripmeester, *Chem. Eur. J*. **1997**, *3*, 1823–1832.

[14] L. J. Prins, C. Thalacker, F. Würthner, P. Timmerman, D. N. Reinhoudt, *Proc. Natl. Acad. Sci*. **2001**, *98*, 10042–10045.

[15] L. J. Prins, K. A. Jolliffe, R. Hulst, P. Timmerman, D. N. Reinhoudt, *J. Am. Chem. Soc*. **2000**, *122*, 3617–3627.

[16] L. J. Prins, J. Huskens, F. de Jong, P. Timmerman, D. N. Reinhoudt, *Nature* **1999**, *398*, 498–502.

[17] J. M. C. A. Kerckhoffs, M. Crego-Calama, I. Luyten, P. Timmerman, D. N. Reinhoudt, *Org. Lett*. **2000**, *2*, 4121–4124.

[18] L. J. Prins, R. Hulst, P. Timmerman, D. N. Reinhoudt, *Chem. Eur. J*. **2002**, *8*, 2288–2301.

[19] Similar forms of cooperativity have been observed for covalent host molecules: S. Shinkai, M. Ikeda, A. Sugasaki, M. Takeuchi, *Acc. Chem. Res*. **2001**, *34*, 494–503.

[20] K. A. Connors, *Binding Constants*, Wiley, New York, **1987**.

[21] The observed positive allosterisms were also analyzed by use of the Scatchard plots, in which Hill coefficients (n) are correlated with the maximum values (y_{max}), according to the equation: $n = 1/(1 - y_{max})$, and the positive and negative allosterisms are expressed by the upward and downward curvatures, respectively. From the plots of y versus $y/[(S)\text{-}\mathbf{2b}]$, y_{max} values were observed at 0.6 ($n = 2.5$ for the first CD change) and at 0.51 ($n = 2.0$ for the second CD change) with upward curvatures (see Supporting Information). For the Scatchard plot see: B. Permutter-Hayman, *Acc. Chem. Res*. **1986**, *19*, 90–96.

[22] The two-step mechanism for the complexation was also corroborated by use of a Job plot (see Supporting Information). The plot of CD values at 305 nm against $[\mathbf{1a}_3\cdot(\mathrm{BuCYA})_6]/([\mathbf{1a}_3\cdot(\mathrm{BuCYA})_6]+[(S)\text{-}\mathbf{2b}])$ has a gentle curvature with a maximum around 0.2, which is attributed to the combination of the two maxima at 0.25 (for 1:3 complex) and 0.143 (for 1:6 complex).

[23] Judging from the acidity of benzyl carboxylic acids ($pK_a \approx 4$) and the basicity of aliphatic amines ($pK_a = 10$–11), ion-pair formation ($NH_3^+/{}^-OOC$) can be expected in the complexation of $\mathbf{1a}_3\cdot(\mathrm{BuCYA})_6$ with **2**. See also C. Reichardt, *Solvents and Solvent Effects in Organic Chemistry*, VCH, Weinheim, Germany, **1990** and R. H. Vreekamp, W.

  1433-7851/02/4111-1928 $ 20.00+.50/0

Verboom, D. N. Reinhoudt, *J. Org. Chem.* **1996**, *61*, 4282 – 4288. Furthermore, in nonpolar solvents such as toluene, the tight ion pair can be the main species. See also E. Yashima, T. Matsushima, Y. Okamoto, *J. Am. Chem. Soc.* **1997**, *119*, 6345 – 6359 and E. Yashima, Y. Maeda, Y. Okamoto, *J. Am. Chem. Soc.* **1998**, *120*, 8895 – 8896.

[24] J. C. Ma, D. A. Dougherty, *Chem. Rev.* **1997**, *97*, 1303 – 1324.

[25] C. A. Deakyne, M. Meot-Ner (Mautner), *J. Am. Chem. Soc.* **1985**, *107*, 474 – 479.

[26] D. A. Rodham, S. Suzuki, R. D. Suenram, F. J. Lovas, S. Dasgupta, W. A. Goddard III, G. A. Blake, *Nature* **1993**, *362*, 735 – 737.

[27] Y. Kikuchi, Y. Tanaka, S. Sutarto, K. Kobayashi, H. Toi, Y. Aoyama, *J. Am. Chem. Soc.* **1992**, *114*, 10302 – 10306.

[28] Additional interaction of an NH_3^+ group with the phenyl group of the neighboring guest moiety by cation – π interactions might also contribute to the observed cooperativity. However, it seems likely that solvent molecules in the first solvation shell play an important role in these interactions, because modeling studies indicate that direct contact between two complexed acid molecules is rather unlikely.

Designed Ligands as Probes for the Catalytic Binding Mode in Mo-Catalyzed Asymmetric Allylic Alkylation**

Barry M. Trost,* Kalindi Dogra, Iwao Hachiya, Takashi Emura, David L. Hughes,* Shane Krska, Robert A. Reamer, Michael Palucki, Nobuyoshi Yasuda, and Paul J. Reider

Asymmetric allylic alkylation has been developing significantly over the past several years.[1] Among the metals capable of effecting such reactions are palladium,[2] molybdenum,[3] and tungsten.[4] In contrast to these metals, in which the chirality of some substrates, notably vinylcarbinols of the type shown in Equation (1), is lost, iridium,[5] rhodium,[6] and ruthenium[7] normally retain the optical purity of such starting substrates. In spite of these many studies, very little is known about the structure of the active complex in the catalytic cycle. The case of Mo is quite intriguing. The catalyst system based on ligand **1**[8] has shown extraordinary levels of regio- and enantioselectivity, even at elevated temperatures (80 – 100 °C) [Eq. (1)].[3a] Furthermore, the reactions were qualitatively significantly faster than in the previously reported achiral reactions.[9] How such a seemingly flat system is able to provide such high selectivities has stimulated the development of an understanding of its binding mode. Although the direct characterization of π-allyl – metal complexes is certainly desirable, the relevance of these isolable/observable complexes to the catalytic cycle is not assured. Herein we adopted an indirect probe of the question of the binding of this ligand to Mo during the catalytic cycle which has led to a totally unexpected result.

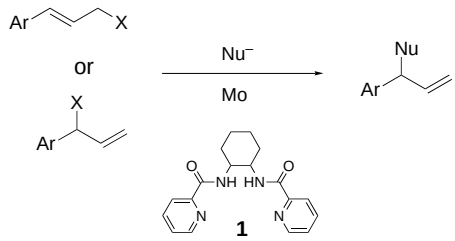

(1)

In the original design, three binding modes **I**—**III** for these octahedral metals were considered. Conceptually, it was postulated that binding mode **I**, while the most common,

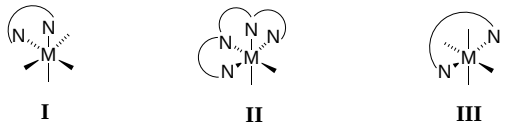

would have less probability of inducing high enantiomeric excesses in asymmetric allylic alkylations than **II** and **III**. The reaction depicted in Equation (2) was employed to evaluate

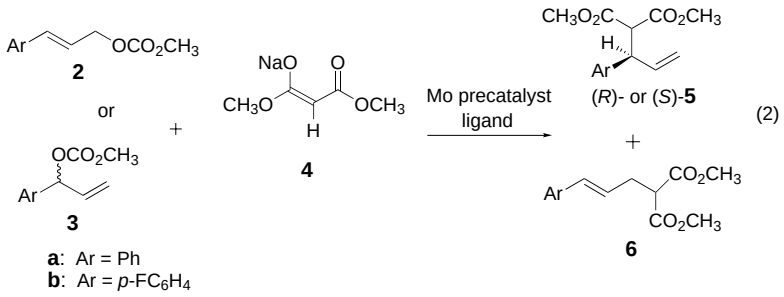

(2)

the ligands. Several ligands were evaluated, and their effectiveness compared with that of **1** as the standard ligand (Table 1, entries 1, 2, and 12).

In initial studies, one of the two picolinamide units was replaced with a nicotinamide group (see **7**). Surprisingly, the regio- and enantioselectivities were slightly better than with the standard ligand **1**, although the reactions were slower (Table 1, entry 3). Since it seemed that the nitrogen atom of the nicotinamide group could not participate in the binding, the simple benzamide ligand **8** was examined. In agreement with the above hypothesis, the reaction of ligand **8** with the achiral substrate **2** (Table 1, entry 4) gave the same results as the reaction of ligand **7** with **2** (Table 1, entry 3). Interestingly, better selectivities were obtained in the reaction of ligand **8** with chiral racemic substrate **3** (Table 1, entry 5) than in the

[*] Prof. B. M. Trost, K. Dogra, Dr. I. Hachiya, T. Emura
Department of Chemistry, Stanford University
Stanford, CA 94305 (USA)
Fax: (+1) 650-725-0002
E-mail: bmtrost@stanford.edu
Dr. D. L. Hughes, Dr. S. Krska, Dr. R. A. Reamer, Dr. M. Palucki, Dr. N. Yasuda, Dr. P. J. Reider
Department of Process Research, Merck Research Laboratories
Rahway, NJ 07065 (USA)
Fax: (+1) 732-594-4717
E-mail: dave_hughes@merck.com

[**] We thank the National Science Foundation and the National Institutes of Health for their generous support of the work carried out at Stanford. I.H. thanks the Japan Society for the Promotion of Science for a postdoctoral fellowship. Mass spectra were provided by the Mass Spectrometry Facility at the University of California, San Francisco, which is supported by the NIH Division of Research Resources.

  1433-7851/02/4111-1929 $ 20.00+.50/0